Zinc transporter 8 haploinsufficiency protects against beta cell dysfunction in type 1 diabetes by increasing mitochondrial respiration

Yong Kyung Kim [1], Jay A. Walters [1], Nicole D. Moss [1], Kristen L. Wells [1,2], Ryan Sheridan [2], Jose G. Miranda [1], Richard K.P. Benninger [1], Laura L. Pyle [1,3], Richard M. O'Brien [4], Lori Sussel [1], Howard W. Davidson [1,5,*]

ABSTRACT

Objective: Zinc transporter 8 (ZnT8) is a major humoral target in human type 1 diabetes (T1D). Polymorphic variants of *Slc30A8*, which encodes ZnT8, are also associated with protection from type 2 diabetes (T2D). The current study examined whether ZnT8 might play a role beyond simply being a target of autoimmunity in the pathophysiology of T1D.

Methods: The phenotypes of NOD mice with complete or partial global loss of ZnT8 were determined using a combination of disease incidence, histological, transcriptomic, and metabolic analyses.

Results: Unexpectedly, while complete loss of ZnT8 accelerated spontaneous T1D, heterozygosity was partially protective. *In vivo* and *in vitro* studies of ZnT8 deficient NOD.SCID mice suggested that the accelerated disease was due to more rampant autoimmunity. Conversely, beta cells in heterozygous animals uniquely displayed increased mitochondrial fitness under mild proinflammatory conditions.

Conclusions: In pancreatic beta cells and immune cell populations, Zn^{2+} plays a key role as a regulator of redox signaling and as an independent secondary messenger. Importantly, Zn^{2+} also plays a major role in maintaining mitochondrial homeostasis. Our results suggest that regulating mitochondrial fitness by altering intra-islet zinc homeostasis may provide a novel mechanism to modulate T1D pathophysiology.

1. INTRODUCTION

Type 1 diabetes (T1D) is an autoimmune disease characterized by T cell mediated destruction of insulin producing beta cells [1]. The triggering event(s) that lead to T1D have not been fully established, but in humans, the development of T1D can be predicted by the presence of two or more islet autoantibodies [2,3]. However, beyond being the targets of adaptive immune responses, functional roles for autoantigens in disease pathophysiology remain uncertain [4—7]. ZnT8 transports Zn^{2+} into the insulin secretory granules of pancreatic beta cells in exchange for protons, which allows the formation of Zn^{2+} insulin crystals [8]. In humans, genetic studies have shown that *SLC30A8* haploinsufficiency protects against Type 2 diabetes (T2D) whereas the interpretation of genome wide association study (GWAS) data is more complex with ZnT8 variants viewed as having either a positive or negative relationship with T2D risk, depending on the risk allele [9]. Additional studies have investigated the importance of ZnT8 for beta cell function, predominantly in the context of glucose metabolism [10], but its functional contribution to T1D has largely been ignored.

To investigate whether ZnT8 contributes to the initiation and/or progression of T1D, we used a speed-congenic approach to transfer a global *Slc30a8* null allele [11] to the NOD background. Surprisingly, while complete loss of ZnT8 accelerated spontaneous T1D, heterozygosity appeared partially protective, particularly in those animals with a more slowly progressing disease. To investigate the relative contributions of the adaptive immune system and target organ to these phenotypes we next generated $ZnT8^{+/-}$ and $ZnT8^{-/-}$ NOD.SCID mice. *In vivo* and *in vitro* studies revealed a potential role for ZnT8 in regulating mitochondrial function under inflammatory conditions, that may in part explain the protective effect of haploinsufficiency.

[1]Barbara Davis Center for Diabetes, University of Colorado Denver Anschutz Medical Campus, Aurora, CO 80045, USA [2]RNA Biology Initiative, Biochemistry and Molecular Genetics Department, University of Colorado Denver Anschutz Medical Campus, Aurora, CO 80045, USA [3]Director Child Health Research Biostatistics Core, Department of Pediatrics, University of Colorado Denver Anschutz Medical Campus, Aurora, CO 80045, USA [4]Department of Molecular Physiology and Biophysics, Vanderbilt University School of Medicine, Nashville, TN, USA [5]Department of Immunology and Microbiology, University of Colorado Denver Anschutz Medical Campus, Aurora, CO 80045, USA

*Corresponding author. Barbara Davis Center for Diabetes, University of Colorado Denver Anschutz Medical Campus, Aurora, CO 80045, USA. E-mail: howard.davidson@cuanschutz.edu (H.W. Davidson).

2. MATERIALS AND METHODS

2.1. Generation of NOD.ZnT8 KO and NOD.SCID.ZnT8 KO mice

NOD mice lacking ZnT8 were generated using a speed congenic approach [12] by breeding C57BL/6 J.ZnT8 knockout (KO) (RRID:MGI:4359886 [13]; and NOD/MrkTac (Taconic) parents. After 8 generations, microsatellite analyses confirmed that all *Idd* loci had been fixed, and mice were subsequently maintained by intercrossing of heterozygous animals. To generate NOD.SCID.ZnT8 KO mice, parental homozygous animals (NOD/MrkTac/ZnT8$^{-/-}$) were bred to NOD.CB17-Prkdcscid/NCrCrl (Charles River Laboratories) mice. The colony was subsequently maintained by crossing progeny that were homozygous at the *Prkdscid* allele and heterozygous at the *Slc30a8* (ZnT8) allele. For disease incidence studies, animals were monitored for up to 40 weeks of age. Blood glucose was measured with a Freestyle Lite glucometer (Abbott laboratories), and diabetes diagnosed following 2 consecutive readings >250 mg/dl.

2.2. Histology

Pancreata were incubated in 10% neutral buffered formalin for 4 h, processed and embedded in paraffin. Tissue sections were either stained with hematoxylin and eosin (H&E), or incubated with primary antibodies: anti-insulin (1:1000, Dako), anti-insulin (1:20, Invitrogen), mouse anti-ZnT8 (1:20) [14] for 16 h at room temperature (RT), followed by Alexa dye-conjugated secondary antibodies: (anti-mouse, 1:200, Invitrogen), (anti-guinea pig, 1:200, Invitrogen), (anti-rabbit, 1:200, Abcam). After washing, nuclei were stained with DAPI (Invitrogen), and sections mounted in Vectashield (Vector Labs). To calculate insulitis scores, 5−10 sections, randomly selected from multiple pancreatic regions from each animal, were examined in a blinded fashion.

2.3. Glucose tolerance test (GTT)

Mice were fasted for 16 h followed by IP injection of 2 g/kg glucose (Sigma−Aldrich). Blood glucose levels were measured with a glucometer (Bayer Contour). Plasma insulin levels were measured by ELISA (ALPCO) in 4 h fasted mice before or 30 min after IP injection with 2 g/kg glucose.

2.4. Islet isolation and proinflammatory cytokine treatment

Pancreata were isolated from 17-week-old mice and digested by Cizyme RI (Vitacyte), followed by Lympholyte 1.1 (Cedarlane) gradient centrifugation. After isolation, islets were incubated in RPMI 1640 containing 10% FBS and penicillin/streptomycin at 37 °C in a gassed incubator overnight. The following day, islets were transferred to fresh medium either with or without a low dose cocktail of 100 pg/ml TNF-α, 150 pg/ml IL-1β, 10 pg/ml IFN-γ. (R&D Systems), incubated at 37 °C for an additional 24 h, then harvested for subsequent analysis.

2.5. Glucose stimulated insulin secretion

For each replicate, 10 islets were hand-picked and incubated for 1 h in Krebs−Ringer Bicarbonate buffer (KRB) supplemented with 0.1% BSA (Fisher Scientific) and 2 mM glucose, followed by a 30 min incubation in KRB supplemented with 2 mM glucose (Low), 20 mM glucose (High) or 2 mM glucose + 20 mM KCl (KCl). Cells and media were harvested, and islets lysed in PBS containing 2% Triton-X100 for hormone extraction. Proinsulin and insulin were measured by ELISA (proinsulin Mercodia; insulin ALPCO), and secretion normalized to insulin content.

2.6. Measurement of oxygen consumption rate (OCR) in islets

OCR was acquired using a Seahorse XF-e96 (Agilent Technologies) [15]. Size-matched isolated islets were incubated with basal assay media (Agilent Technologies), split into 10 islets per well and plated in poly-D-lysine coated spheroid culture microplates (Agilent), then pre-incubated for 1 h at 37 °C without CO_2 in assay media supplemented with 3 mM glucose and 0.1% FBS (Invitrogen) to optimize respiratory conditions. Glucose (20 mM, Sigma−Aldrich) was added to stimulate the cells and 4 μM oligomycin (Sigma−Aldrich) injected to inhibit ATP synthase. The mitochondrial respiration uncoupler FCCP (4 μM, Sigma−Aldrich) was injected to determine electron transport capacity. To terminate the assay, 4 μM rotenone (Thermo Fisher) was added to block electron transport. Values for basal respiration, maximal capacity, proton leak, and ATP production were calculated with Wave 4.0 software (Agilent).

2.7. Intracellular calcium imaging and analysis

Islets were incubated with 4 μM Fluo-4 AM (ThermoFisher) for 2 h at room temperature in BMHH buffer (125 mM NaCl, 5.7 mM KCl, 2.5 mM $CaCl_2$, 1.2 mM $MgCl_2$, 10 mM HEPES for 1 L, pH 7.4) with 2.8 mM glucose. Images were acquired at 1 frame/s for 5 min after stimulation with 11 mM glucose for 15 min. The intensity of the fluorescence in the whole islets was measured by laser scanning microscopy (LSM 800, Zeiss, Germany) and analyzed with Fiji software. The experiments were repeated independently in triplicate.

2.8. RNA-sequencing

RNA was isolated with the RNeasy Micro kit (QIAGEN). Sequencing (28−36 M reads/sample) was performed using an Illumina Nova-SEQ6000. Reads were aligned to the GRCm38 genome using STAR (version 2.5.2a), then counted using FeatureCounts from the subread package (version 1.6.2). Differential expression analysis was performed using DESeq2 (version 1.30). Splicing analysis was performed using rMATS (version 4.1.2). The full analysis pipeline as well as the results are available at https://github.com/CUAnschutzBDC/ZNT8_analysis.git

2.9. Statistics

Data was processed using Prism 9 (GraphPad Software, San Diego, CA). All values are expressed as the mean ± standard error of mean (SEM). Survival curves were analyzed using a Log-rank (Mantel−Cox) test. Two-tailed Student's *t* tests, Mann−Whitney U tests, and 2-Way ANOVA were used to compare grouped data. For ANOVAs models with and without an interaction term were run. Where no significant genotype:treatment interaction was observed variances for the alternate model are reported.

3. RESULTS

3.1. Acceleration of type 1 diabetes in ZnT8 knockout NOD mice

To investigate the role of ZnT8 in type 1 diabetes (T1D) we generated NOD. ZnT8 knockout mice using a speed congenic approach [12]. Immunofluorescence analysis confirmed the absence of ZnT8 protein expression in the pancreatic islets of the NOD. ZnT8 null (KO) mice, and presence in NOD. ZnT8 heterozygote (HE) and wildtype (WT) controls (Figure 1A). To assess whether deletion of ZnT8 altered susceptibility to spontaneous diabetes, male and female mice were monitored for persistent hyperglycemia for up to 10 months. Surprisingly, female NOD. ZnT8 KO mice (n = 33) developed T1D more rapidly than NOD. ZnT8 WT (n = 40; *p* = 0.003) or NOD. ZnT8 HE (n = 46; *p* < 0.0001) animals (Figure 1B). Male mice had a much lower overall disease incidence, but a similar trend of accelerated disease was observed during the initial 150 d of the study (KO, n = 45 v HE, n = 42; *p* = 0.058; Supplementary Figure 1). To confirm this unexpected
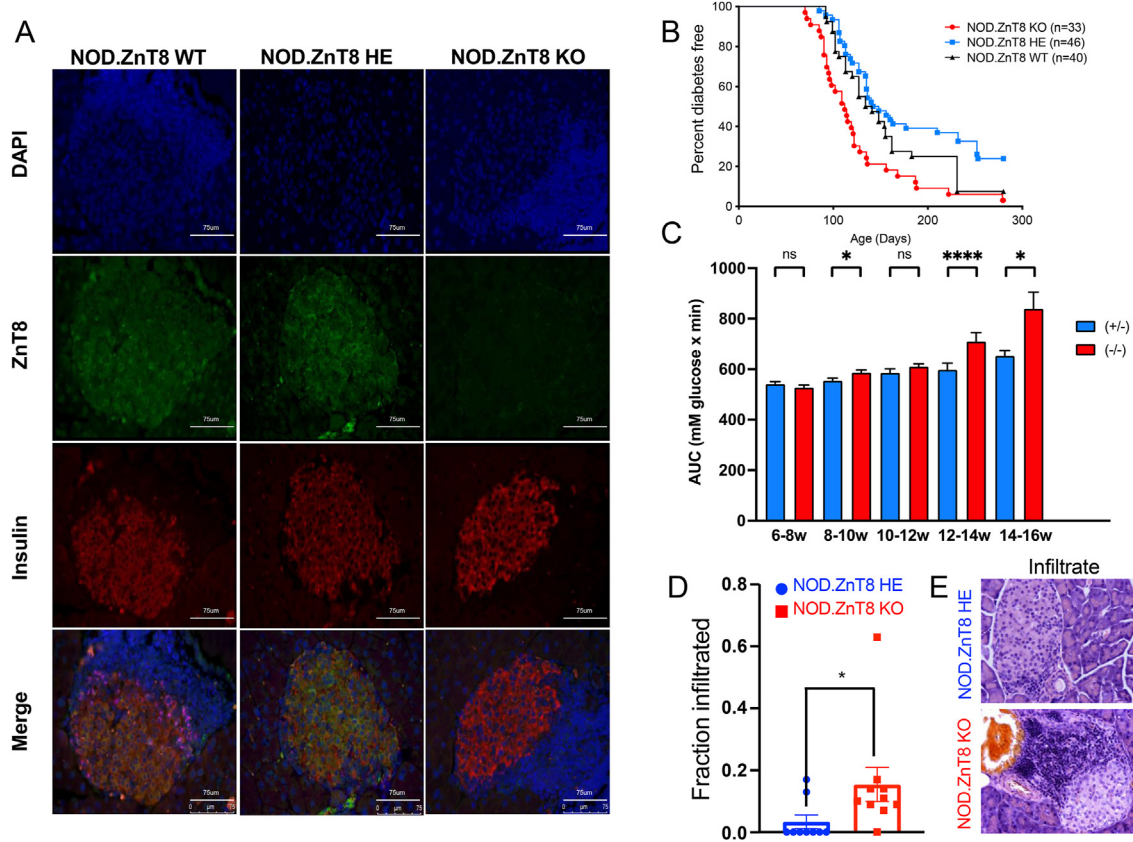
Figure 1: Acceleration of type 1 diabetes in NOD. ZnT8 knockout mice. (A) Representative islet images using immunofluorescent staining of DAPI (blue), ZnT8 (green), and insulin (red) from 12wk NOD. ZnT8 wild-type mice and 7wk NOD. ZnT8 Heterozygote and NOD. ZnT8 knockout mice. Scale bars: 75 μm. (B) Female mice were monitored for the appearance of spontaneous T1D. Median survival was 112 days (KO), 145 days (HE, $p < 0.001$ vs KO), and 137.5 days (WT, $p = 0.0113$ vs KO, 0.046 vs HE). Incidence was 97% (KO), 76% (HE), and 93% (WT) by 40 weeks. (C) Age dependent intraperitoneal glucose tolerance test (IPGTT) after 16 h fasting. HE (blue) and KO (red). (6∼8wks: n = 30 KO, n = 36 HE; 8−10wks: n = 43 KO, n = 46 HE; 10−12wks: n = 36 KO, n = 30 HE; 12−14wks: n = 50 KO, n = 45 HE; 14−16wks: n = 33 KO, n = 25 HE). Data are expressed as the mean ± SEM. $*p < 0.05$, $****p < 0.0001$; Mann−Whitney U test. (D, E) H & E stained pancreas sections from 7 to 8wk NOD. ZnT8 HE and NOD. ZnT8 KO mice were examined in a blinded fashion for evidence of insulitis. (D) 111 islets from 9 NOD. ZnT8 HE mice and 398 islets from 10 NOD. ZnT8 knockout mice were examined. The frequency of islets with any evidence of insulitis was calculated. Data are expressed as the mean ± SEM. $*p = 0.02$; Mann−Whitney U test. (E) Representative H&E images of the most highly infiltrated islets from HE (upper) and KO (lower) animals.

observation, and gain further insight into a potential mechanism, we conducted repeated glucose tolerance tests and histological analyses on an independent cohort of female HE and KO animals (Figure 1C−E). Consistent with our previous observations, at early time points pre-diabetic female NOD. ZnT8 KO mice showed greater glucose intolerance compared to age-matched NOD. ZnT8 HE animals. This was particularly evident at 12−14 weeks (KO, n = 50, HE, n = 45; $p < 0.0001$; Figure 1C), when frank diabetes is also first detected in our colony (Figure 1B).

Groups of 5−10 pre-diabetic HE and KO animals were sacrificed at ∼2 week intervals from 6 to 16 weeks for histological analysis of insulitis. Beyond 10 weeks there were no significant differences between genotypes in the extent or composition of lesions of normoglycemic animals (data not shown). However, consistent with the more rapid T1D onset in KO animals, in early pre-diabetes (6−8 weeks) lymphocytic infiltration was significantly advanced in young female NOD. ZnT8 KO mice compared to age-matched NOD. ZnT8 HE mice (Figure 1D). Thus, at this time point only 2/9 HE animals showed any detectable evidence of insulitis, compared to 9/10 KO animals (Figure 1D; $p = 0.02$). Moreover, although the low numbers precluded accurate quantification of an average insulitis grade, in the 2 HE animals where significant

insulitis was detected it appeared less florid (Figure 1E upper panel), with infiltrates that encompassed >30% of the islet (Figure 1E lower panel) that typically comprised 10−20% of those detected in the KO animals at this time point, being entirely absent. The low numbers of infiltrating cells in young HE animals also precluded more detailed analysis, however, flow cytometry of the infiltrates from late pre-diabetic HE and KO animals did not reveal any significant genotype-related changes in the relative frequencies of the major immune cell sub-types, nor of insulin tetramer positive CD4$^+$ cells (data not shown). Together our results suggest that complete, but not partial, loss of ZnT8 accelerates autoimmunity without altering the fundamental mechanism, perhaps by rendering NOD beta cells more sensitive to inflammatory stressors, and/or by facilitating a more "immunogenic" intra-islet environment that promotes destructive insulitis.

3.2. Low-dose proinflammatory cytokine treatment improves insulin secretion from NOD.SCID ZnT8 HE islets

T1D is characterized by considerable temporal heterogeneity in both NOD mice and humans. Evidence suggests that disease involves both extrinsic and intrinsic mechanisms of beta cell loss, likely including both direct immune mediated destruction and beta cell death following
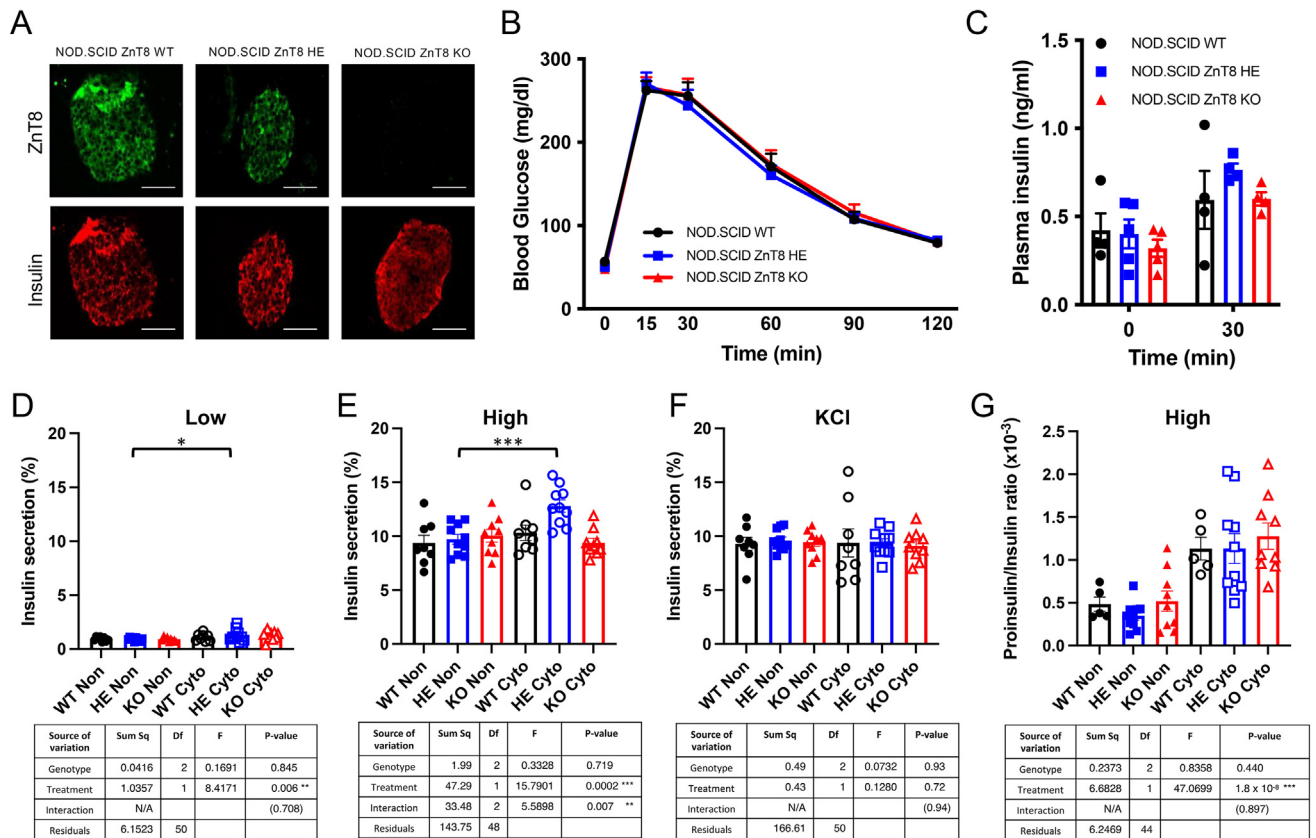
Figure 2: Low dose proinflammatory cytokines improved insulin secretion in NOD.SCID ZnT8 HE isolated islets. (A) Representative images of immunofluorescent staining of ZnT8 (green) and insulin (red) from 17wk NOD.SCID ZnT8 male mice. Scale = 100 μm. (B) Intraperitoneal glucose tolerance test (IPGTT) of 14wk male NOD.SCID WT, HE and KO mice after 16 h fasting and 2 g/kg glucose load by IP injection; n = 9 per group. (C) *In vivo* glucose stimulated insulin secretion measured after 4 h fasting; n = 4 per group. (D—F) *Ex vivo* glucose stimulated insulin secretion assay normalized to insulin content (n = 8—10 per group). (G) The ratio of secreted proinsulin to insulin in response to 20 mM glucose stimulation. Supernatants were collected 30 min after glucose stimulation. Data are expressed as the mean ± SEM, and analyzed by 2-Way ANOVA * $p < 0.05$, ***$p < 0.001$.

unsuccessful adaptive responses to chronic inflammation and latent dysglycemia. Unexpectedly, despite the apparent acceleration of disease in the KO animals, the NOD. ZnT8 HE mice that remained diabetes free for greater than 20 weeks (n = 24) showed increased longevity compared to NOD. ZnT8 WT controls (n = 20; $p = 0.009$) (Figure 1B). This result is consistent with the protective effects seen in a prior study that used shRNAi to partially knockdown ZnT8 in WT NOD mice [16]. The unexpected differences in autoimmune susceptibility between mice with complete or partial ZnT8 loss suggests that ZnT8 haploinsufficiency may have beneficial effects on beta cell function under inflammatory conditions that are masked by the robust adaptive immune response in the KO animals. To eliminate the potentially confounding influence of autoreactive T and B lymphocytes, we generated ZnT8 KO and HE mice on the NOD.SCID background and confirmed the absence of ZnT8 protein in the NOD.SCID ZnT8 KO animals (Figure 2A). At 15 weeks of age, male and female NOD.SCID ZnT8 HE and NOD.SCID ZnT8 KO mice had normal body weights compared to the NOD.SCID ZnT8 WT controls (Supplemental Figure 2A-B) and did not display dysregulated glucose tolerance or *in vivo* plasma insulin secretion under basal conditions (Figure 2B—C, Supplemental Figure 2C-D). Furthermore, there were no detectable *in vitro* insulin

secretion defects in control islets isolated from NOD.SCID ZnT8 HE and NOD.SCID ZnT8 KO animals of either gender compared to NOD.SCID ZnT8 WT littermate controls (Figure 2B—C, Supplemental Figure 2E). Such data is consistent with findings on other genetic backgrounds [10] and reinforces the idea that the accelerated disease observed in the NOD. ZnT8 KO animals results from a direct effect on adaptive immunity.

To investigate whether beta cell function was directly affected by loss or reduction of ZnT8 in a controlled inflammatory environment, NOD.SCID ZnT8 WT, HE, and KO islets from male mice were treated for 24 h with a low-dose cocktail of proinflammatory cytokines (100 pg/ml TNF-α, 150 pg/ml IL-1β, 10 pg/ml IFN-γ); concentrations that do not cause overt cell death in WT NOD.SCID islets, and are comparable to human circulating levels [17]. Interestingly, while cytokine-treated NOD.SCID ZnT8 WT and NOD.SCID ZnT8 KO islets showed no differences in low or high glucose stimulated insulin secretion compared to untreated islets (Figure 2D,E), cytokine treatment of NOD.SCID ZnT8 HE islets significantly increased both basal and glucose stimulated insulin secretion (GSIS) (Figure 2D,E, $p = 0.036$ [low]; $p = 0.0002$ [high]), suggesting that moderately reduced levels of ZnT8 actually improved beta cell function under mild inflammatory conditions. Insulin
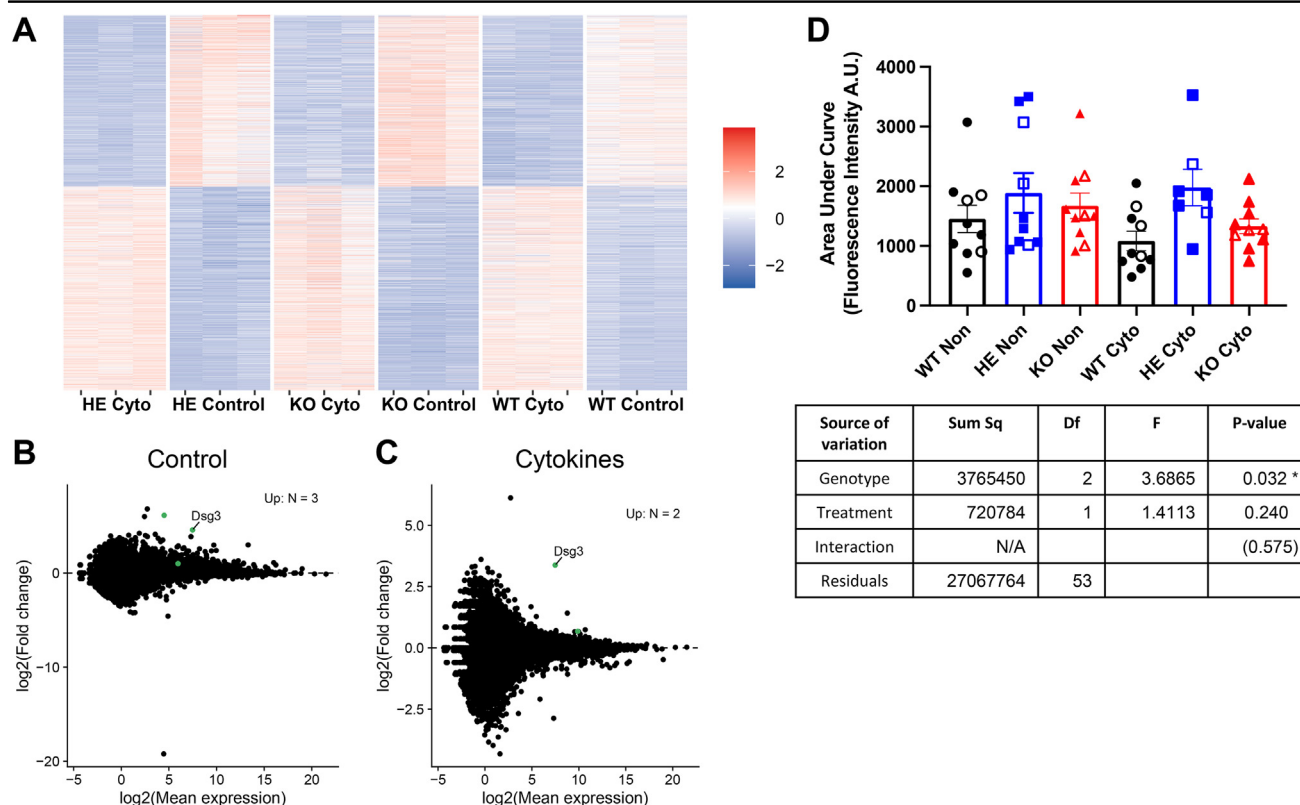
Figure 3: Differentially regulated gene expression and increased calcium oscillations in islets treated with proinflammatory cytokines. (A–C) RNA-Seq analysis of 17 wks NOD.SCID.ZnT8 WT, HE and KO male islets; untreated and treated with proinflammatory cytokines for 24 h, N = 3 per group. Because WT and KO had similar phenotypes, these were averaged for differential expression analysis with DESeq2 (version 1.30.0). Differentially expressed genes were identified using the DESeq function with default parameters and genes for the comparison of the HE islets vs the average of the WT and KO islets were identified using the results function [results (contrast = list (HE_sample, c (WT_sample, KO_sample)), listValues = c (1, −1/2)]. (A) Heatmap of differentially expressed genes in individual replicates. (B, C) Differential expression analysis comparing averaged NOD.SCID.ZnT8 WT and KO with HE islets under control (B) and cytokine (C) conditions. Up-regulated genes with pAdj <0.05 are shown in green (n = 3 [control], n = 2 [cytokine]). (D) Islets (7—10 per group derived from 4 mice of each genotype (3 male and 1 female) were incubated for 24 h with or without proinflammatory cytokines, then loaded with a Fluo-4AM calcium indicator and imaged during stimulation with 11 mM glucose. The area under the curve for each islet is shown. Islets from male mice are shown as solid symbols and females as open symbols. 2-Way ANOVA was used to compare groups.$*p < 0.05$.

content was unchanged in any of the isolated islet samples in both untreated and cytokine treated conditions (Supplemental Figure 2F). The ratio of secreted proinsulin to insulin was significantly increased by cytokine treatment ($p < 0.0001$), but this was independent of genotype (Figure 2G).

3.3. Partial ZnT8 knockdown does not result in gross changes to the islet transcriptome

To begin to investigate the mechanism(s) responsible for the observed improved function of HE beta cells we first analyzed global transcriptomes of control versus cytokine treated islets. As expected, cytokine treatment led to significant transcriptional changes (Figure 3A) that were primarily associated with pathways involving stress responses and cell death (Supplemental Figure 3A). However, the samples clustered based on treatment group rather than genotype (Supplemental Figure 3B) and no obvious gene expression changes between the different genetic backgrounds that would explain the phenotypic behavior were observed. Thus, after correction for multiple comparisons only 3 genes showed significant up-regulation in control HE islets compared to the other 2 genotypes (Figure 3B). Similarly, only 2 genes were up-regulated in cytokine treated HE islets relative to treated islets from the other 2 strains (Figure 3C), including Dsg3, a gene that encodes the Desmosomal cadherin desmoglein 3, which

was also up-regulated in the control islets (Figure 3B). There were also no significant genotype-dependent differences in alternative splicing (Supplemental Figure 3C).

3.4. NOD.SCID ZnT8 HE mice islets display improved mitochondrial function under inflammatory conditions

Like other electrically coupled secretory events, GSIS involves Ca^{2+} influx. Thus, we next examined calcium fluxes in control versus cytokine treated islets. Consistent with their enhanced ability to secrete insulin, NOD.SCID ZnT8 HE islets displayed significantly increased calcium oscillations in response to glucose stimulation compared to WT, but not KO, islets that was independent of cytokine treatment ($p = 0.025$ v WT; $p = 0.21$ v KO; Figure 3D, Supplemental Figure 4). Mitochondria play critical roles in regulating Ca^{2+} homeostasis, and mitochondrial dysfunction has been implicated in T1D pathogenesis, both as a cause of altered immune cell activity [18] and the source of excess reactive oxygen species (ROS) that can induce and/or potentiate oxidative stress [19,20]. Importantly, Zn^{2+} plays a major role in maintaining mitochondrial homeostasis, and dynamic regulation of mitochondrial Zn^{2+} is essential for normal cellular metabolism [21]. Thus, we assessed mitochondrial function in islets from NOD.SCID ZnT8 WT, NOD.SCID ZnT8 HE and NOD.SCID ZnT8 KO mice under basal and cytokine treated conditions. Analysis using the Seahorse
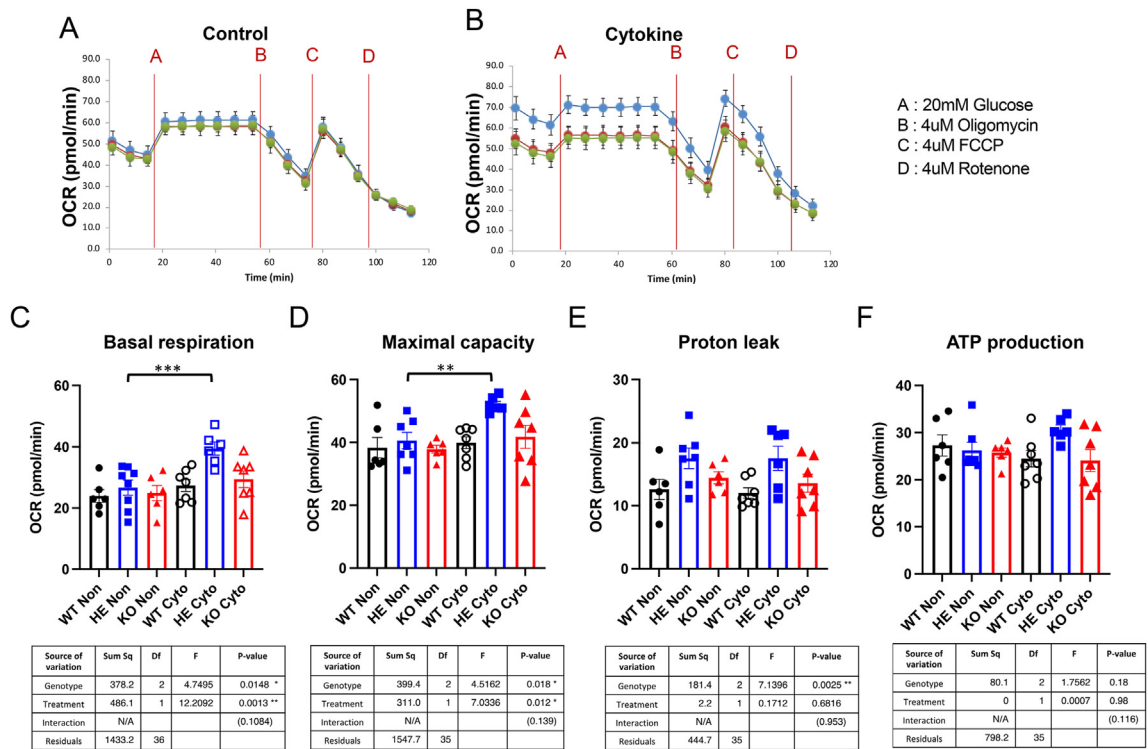
Figure 4: Increased oxygen consumption rate (OCR) upon low dose proinflammatory cytokine treatment in NOD.SCID HE male isolated islets. (A) Representative oxygen consumption rate (OCR) analysis in isolated islets without cytokine treatment and (B) treated with low dose cytokine for 24 h. From each animal 10 size-matched islets per well were analyzed in Seahorse XFe-96 spheroid plates. Islets were acutely exposed to A: 20 mM glucose, B: 4 µM Oligomycin, C: 4 µM FCCP, D: 4 µM Rotenone. n = 7 WT, n = 6 HE and n = 7 KO. Green circle = WT, blue circle = HE and black = KO. (C−F) Basal respiration, maximal respiration, proton leak and ATP production was calculated by Wave 4.0 software. Data are expressed as the mean ± SEM and analyzed by 2-Way ANOVA **$p < 0.01$, ***$p < 0.001$.

metabolic analyzer revealed that under basal conditions oxygen consumption rates (OCR) were identical in male and female animals of all 3 strains (Figure 4A,C, Supplemental Figure 5A, C). However, in contrast to the WT and KO mice low levels of proinflammatory cytokines significantly increased basal respiration in islets from the HE animals (Figure 4B,C, Supplemental Figure 5B, C, Supplemental Table 1; $p = 0.0004$ [males], $p = 0.004$ [females]). Cytokine treatment also increased the maximal capacity of islets from male but not female, HE mice (Figure 4D, Supplemental Figure 5D; $p = 0.003$ [males], $p = 0.169$ [females]). Independent of cytokine treatment male HE islets showed significantly higher proton leak than those from the other genotypes (Figure 4E, Supplemental Figure 5E; $p = 0.002$ v WT, $p = 0.044$ v KO), suggesting that uncoupling of basal respiration from ATP production might contribute to the improved cellular respiration. There was also a trend towards possible cytokine induced increases in ATP production by HE islets (Figure 4F, Supplemental Figure 5F; $p = 0.096$ [males], $p = 0.099$ [females]) that in females but not males, contrasted with a trend towards cytokine induced decreased ATP production by KO islets ($p = 0.514$ [males], $p = 0.062$ [females]) (Supplemental Table 1). Together, these results suggest that partial, but not complete reduction of ZnT8, perhaps through the optimal dynamic modulation of cytoplasmic $[Zn^{2+}]$, provides a bioenergetic advantage to beta cells in proinflammatory conditions.

4. DISCUSSION

To investigate the role of ZnT8 in T1D, we generated ZnT8 mutant NOD mice, anticipating that animals lacking ZnT8 might display improved

beta cell survival due to the role of ZnT8 as an autoantigen. Contrary to this prediction, diabetes onset was actually accelerated, suggesting that ZnT8 has a previously unanticipated and likely indirect, tolerogenic role in these animals. The observed absence of any protective effect of complete ZnT8 KO is consistent with previous observations, that unlike many humans, but similar to the IA-2 autoantigen [22], ZnT8 is only a minor target of autoimmunity in NOD mice [23]. However, our results contrast strongly with those from NOD mice with KO of other T1D autoantigens such as GAD65, IA-2 or IGRP, that each show WT rates of progression [7,24,25]. Unlike the KO animals, diabetes was partially attenuated in NOD. ZnT8 HE mice, suggesting that HE beta cells may be more resistant to prolonged low level inflammation than those of the WT animals. This result is in apparent agreement with a recent study showing protection of C57BL/6 J ZnT8HE and KO mice from diet induced obesity [26], given that the exaggerated autoimmunity in the NOD ZnT8KO animals may mask any protective effect of the KO on β cell function in response to low grade inflammation.

To allow direct analysis of β cell function without the potentially confounding influence of concurrent autoimmunity we transferred the ZnT8KO to the NOD.SCID background. In a more controlled inflammatory environment, isolated islets from NOD.SCID mice carrying a heterozygous mutation of *Slc30a8* showed improved mitochondrial fitness, a feature that likely contributes to their improved survival in the chronic NOD autoimmune environment [27]. Surprisingly, however, under identical conditions ZnT8 KO mice did not display a similar improvement in mitochondrial function. Insulin secretion and cytoplasmic $[Zn^{2+}]$ are coupled in a highly dynamic process linked to redox changes in the cell [8] and we suspect that the difference between the

HE and KO animals is most likely due to adaptive compensatory changes that limit the ability of the KO animals to induce the protective response seen in the HE mice which might itself involve gender-specific mechanisms. This may also explain possible functional differences between KO β cells in our study and those in studies employing RNAi based KO of ZnT8 [16,28]. While as expected, cytokine treatment led to significant transcriptional changes, we did not detect a signature that would explain the distinct metabolic response to cytokines of the HE islets. This suggests that the observed enhanced secretory function of HE beta cells likely reflects translational or post-translational changes. As discussed above, T2D in humans is associated with a chronic low-grade inflammation, and we speculate that islets from individuals with protective polymorphic ZnT8 variants may likewise show improved mitochondrial fitness upon cytokine exposure. Future studies will be devoted to testing these hypotheses.

There is increasing evidence that T1D in both humans and mice is preceded by signs of endoplasmic reticulum (ER) stress [29,30]. Moreover, it has been reported that down-regulation of ZnT8 can protect human fetal insulinoma cells from cytokine-induced damage by promoting the unfolded protein response [28]. Thus it is perhaps surprising that we did not detect any significant basal or induced differences in markers of ER stress between NOD.SCID ZnT8WT, HE, and KO islets. It should, of course, be noted that unlike Merriman and Fu [28] we deliberately chose cytokine concentrations that did not induce significant cell death during the time course of our experiments in an effort to more accurately mimic chronic rather than acute inflammation. Thus, we cannot exclude the possibility that a similar phenotype to that previously reported might be evident in NOD ZnT8KO islets treated with nanomolar rather than picomolar concentrations of cytokines. However, it is also possible that the effects of ZnT8 KO on susceptibility to ER stress observed in the prior study might be mechanistically linked to differences in mitochondrial fitness, which was not measured. There is increasing awareness of the fundamental importance of mitochondria-ER contact sites in the regulation of calcium homeostasis, autophagy, apoptosis, and lipid synthesis [31,32]. In particular, deregulation of ER-mitochondrial Ca^{2+} transfer, that itself is influenced by the redox state of the cell, is associated with many pathological conditions, including T2D [31]. Ca^{2+} fluxes across the inner mitochondrial membrane are critical to ATP synthesis and maintaining optimal cellular bioenergetic responses to changing demand [32]. Thus, the increased GSIS in the cytokine treated HE islets likely reflects improved Ca^{2+} dynamics in these organelles, which may in turn indicate a heightened ability to buffer Ca^{2+} under conditions of oxidative ER stress. Although direct analysis of the influence of ZnT8 on Ca^{2+} fluxes across the inner mitochondrial membrane was beyond the scope of the current study, we speculate that this is central to the phenotypes we observe, and that the complex interplay between cellular Zn^{2+}, ROS, and Ca^{2+} fluxes in β cells creates a "Goldilocks" effect, such that ZnT8HE islets are more able to maintain optimal intra-islet cation dynamics in the context of proinflammatory conditions, exhibiting greater resilience to low grade stress than either the WT or KO β cells.

At present, the underlying mechanism for the accelerated disease in immunocompetent NOD. ZnT8KO mice remains uncertain, with at least three potential explanations being plausible; (1) the complete loss of ZnT8 increases β cell "immunogenicity"; (2) ZnT8 is a major target of I–A^{g7} restricted regulatory T cells; or (3) the Zn^{2+} normally co-secreted with insulin creates a more tolerogenic intra-islet environment by impacting signaling in innate and/or adaptive immune cells [33,34]. Although defining a precise mechanism was beyond the scope of the current study, of these possibilities we favor the third. Thus, we did not detect any significant genotype-specific differences in markers of ER stress that might indicate increased generation of post-translationally modified "neo-antigens" that would render the KO cells more immunogenic [35]. Similarly, we are unaware of any evidence that ZnT8 is expressed in NOD thymic epithelial cells, or that it is indeed a significant target of I–A^{g7} restricted regulatory T cells [23]. Conversely, there is abundant evidence that co-secreted Zn^{2+} has autocrine, paracrine, and endocrine roles, both locally in islets, and in the organism as a whole [36], and that local ionic and metabolic environments are critical to promoting, or restraining, immune responses in tissues, as evidenced by the presence of "hot" or "cold" tumors [37]. A potential limitation to our study is that it focused exclusively on a single background strain of mice (NOD). Previous studies of the effects of ZnT8 KO have shown disparities between the phenotypes observed in mice of different genetic backgrounds [10]. Thus it is possible that some of the results we report are strain specific. At present NOD mice are the only well-established mouse model of spontaneous T1D (our primary focus), but an important future direction of the project will be to investigate the influence of ZnT8 on other T1D models, and to extend our studies of low level cytokine treatment to non-autoimmune strains of mice for direct comparison.

AUTHOR CONTRIBUTIONS

Y.K.K. and J.A.W. researched data. Y.K.K., N.D.M., K.L.W., R.S., J.G.M., L.L.P., and H.W.D. analyzed data. Y.K.K., L.S., and H.W.D wrote the manuscript. J.G.M., R.K.P.B., and R.M.O'B. contributed to discussion and edited the manuscript. H.W.D. is the guarantor of this work and, as such, had full access to all the data in the study and takes responsibility for the integrity of the data and the accuracy of the data analysis.

DATA AVAILABILITY

Data will be made available on request.

ACKNOWLEDGEMENTS

CONFLICT OF INTEREST

None.

APPENDIX A. SUPPLEMENTARY DATA

Supplementary data to this article can be found online at https://doi.org/10.1016/j.molmet.2022.101632.

REFERENCES

[1] Eisenbarth, G.S., 1986. Type I diabetes mellitus. A chronic autoimmune disease. The New England Journal of Medicine 314(21):1360–1368.

[2] Boldison, J., Wong, F.S., 2016. Immune and pancreatic beta cell interactions in type 1 diabetes. Trends in Endocrinology and Metabolism 27(12):856–867.

Brief Communication

[3] Ziegler, A.G., Rewers, M., Simell, O., Simell, T., Lempainen, J., Steck, A., et al., 2013. Seroconversion to multiple islet autoantibodies and risk of progression to diabetes in children. JAMA 309(23):2473—2479.

[4] Achenbach, P., Lampasona, V., Landherr, U., Koczwara, K., Krause, S., Grallert, H., et al., 2009. Autoantibodies to zinc transporter 8 and SLC30A8 genotype stratify type 1 diabetes risk. Diabetologia 52(9):1881—1888.

[5] Moriyama, H., Abiru, N., Paronen, J., Sikora, K., Liu, E., Miao, D., et al., 2003. Evidence for a primary islet autoantigen (preproinsulin 1) for insulitis and diabetes in the nonobese diabetic mouse. Proceedings of the National Academy of Sciences of the United States of America 100(18):10376—10381.

[6] Thebault-Baumont, K., Dubois-Laforgue, D., Krief, P., Briand, J.P., Halbout, P., Vallon-Geoffroy, K., et al., 2003. Acceleration of type 1 diabetes mellitus in proinsulin 2-deficient NOD mice. Journal of Clinical Investigation 111(6):851—857.

[7] Yamamoto, T., Yamato, E., Tashiro, F., Sato, T., Noso, S., Ikegami, H., et al., 2004. Development of autoimmune diabetes in glutamic acid decarboxylase 65 (GAD65) knockout NOD mice. Diabetologia 47(2):221—224.

[8] Chabosseau, P., Rutter, G.A., 2016. Zinc and diabetes. Archives of Biochemistry and Biophysics 611:79—85.

[9] Barragan-Alvarez, C.P., Padilla-Camberos, E., Diaz, N.F., Cota-Coronado, A., Hernandez-Jimenez, C., Bravo-Reyna, C.C., et al., 2021. Loss of Znt8 function in diabetes mellitus: risk or benefit? Molecular and Cellular Biochemistry 476(7):2703—2718.

[10] Davidson, H.W., Wenzlau, J.M., O'Brien, R.M., 2014. Zinc transporter 8 (ZnT8) and beta cell function. Trends in Endocrinology and Metabolism 25(8):415—424.

[11] Pound, L.D., Sarkar, S.A., Benninger, R.K., Wang, Y., Suwanichkul, A., Shadoan, M.K., et al., 2009. Deletion of the mouse Slc30a8 gene encoding zinc transporter-8 results in impaired insulin secretion. Biochemical Journal 421(3):371—376.

[12] Rogner, U.C., Avner, P., 2003. Congenic mice: cutting tools for complex immune disorders. Nature Reviews Immunology 3(3):243—252.

[13] Pound, L.D., Sarkar, S.A., Ustione, A., Dadi, P.K., Shadoan, M.K., Lee, C.E., et al., 2012. The physiological effects of deleting the mouse SLC30A8 gene encoding zinc transporter-8 are influenced by gender and genetic background. PLoS One 7(7):e40972.

[14] Pound, L.D., Hang, Y., Sarkar, S.A., Wang, Y., Milam, L.A., Oeser, J.K., et al., 2011. The pancreatic islet beta-cell-enriched transcription factor Pdx-1 regulates Slc30a8 gene transcription through an intronic enhancer. The Biochemical Journal 433(1):95—105.

[15] Taddeo, E.P., Stiles, L., Sereda, S., Ritou, E., Wolf, D.M., Abdullah, M., et al., 2018. Individual islet respirometry reveals functional diversity within the islet population of mice and human donors. Molecular Metabolism 16:150—159.

[16] Sun, H., Li, C., Li, S., Li, X., Wang, J., Zhou, Z., et al., 2018. Gene silencing of ZnT8 attenuates inflammation and protects pancreatic tissue injury in T1D. Immunology Letters 198:1—6.

[17] Dula, S.B., Jecmenica, M., Wu, R., Jahanshahi, P., Verrilli, G.M., Carter, J.D., et al., 2010. Evidence that low-grade systemic inflammation can induce islet dysfunction as measured by impaired calcium handling. Cell Calcium 48(2—3):133—142.

[18] Chen, J., Chernatynskaya, A.V., Li, J.W., Kimbrell, M.R., Cassidy, R.J., Perry, D.J., et al., 2017. T cells display mitochondria hyperpolarization in human type 1 diabetes. Science Report 7(1):10835.

[19] Chen, J., Stimpson, S.E., Fernandez-Bueno, G.A., Mathews, C.E., 2018. Mitochondrial reactive oxygen species and type 1 diabetes. Antioxidants & Redox Signaling 29(14):1361—1372.

[20] Vig, S., Lambooij, J.M., Zaldumbide, A., Guigas, B., 2021. Endoplasmic reticulum-mitochondria crosstalk and beta-cell destruction in type 1 diabetes. Frontiers in Immunology 12:669492.

[21] Wang, X., An, P., Gu, Z., Luo, Y., Luo, J., 2021. Mitochondrial metal ion transport in cell metabolism and disease. International Journal of Molecular Sciences 22(14):7525.

[22] Bonifacio, E., Atkinson, M., Eisenbarth, G., Serreze, D., Kay, T.W., Lee-Chan, E., et al., 2001. International Workshop on Lessons from Animal Models for Human Type 1 Diabetes: identification of insulin but not glutamic acid decarboxylase or IA-2 as specific autoantigens of humoral autoimmunity in nonobese diabetic mice. Diabetes 50(11):2451—2458.

[23] Nayak, D.K., Calderon, B., Vomund, A.N., Unanue, E.R., 2014. ZnT8-reactive T cells are weakly pathogenic in NOD mice but can participate in diabetes under inflammatory conditions. Diabetes 63(10):3438—3448.

[24] Kubosaki, A., Miura, J., Notkins, A.L., 2004. IA-2 is not required for the development of diabetes in NOD mice. Diabetologia 47(1):149—150.

[25] Oeser, J.K., Parekh, V.V., Wang, Y., Jegadeesh, N.K., Sarkar, S.A., Wong, R., et al., 2011. Deletion of the G6pc2 gene encoding the islet-specific glucose-6-phosphatase catalytic subunit-related protein does not affect the progression or incidence of type 1 diabetes in NOD/ShiLtJ mice. Diabetes 60(11):2922—2927.

[26] Syring, K.E., Bosma, K.J., Goleva, S.B., Singh, K., Oeser, J.K., Lopez, C.A., et al., 2020. Potential positive and negative consequences of ZnT8 inhibition. Journal of Endocrinology 246(2):189—205.

[27] Kim, Y.K., Sussel, L., Davidson, H.W., 2021. Inherent beta cell dysfunction contributes to autoimmune susceptibility. Biomolecules 11(4):512.

[28] Merriman, C., Fu, D., 2019. Down-regulation of the islet-specific zinc transporter-8 (ZnT8) protects human insulinoma cells against inflammatory stress. Journal of Biological Chemistry 294(45):16992—17006.

[29] Engin, F., Yermalovich, A., Nguyen, T., Hummasti, S., Fu, W., Eizirik, D.L., et al., 2013. Restoration of the unfolded protein response in pancreatic beta cells protects mice against type 1 diabetes. Science Translational Medicine 5(211):211ra156.

[30] Tersey, S.A., Nishiki, Y., Templin, A.T., Cabrera, S.M., Stull, N.D., Colvin, S.C., et al., 2012. Islet beta-cell endoplasmic reticulum stress precedes the onset of type 1 diabetes in the nonobese diabetic mouse model. Diabetes 61(4):818—827.

[31] Barazzuol, L., Giamogante, F., Cali, T., 2021. Mitochondria associated membranes (MAMs): architecture and physiopathological role. Cell Calcium 94:102343.

[32] Lim, D., Dematteis, G., Tapella, L., Genazzani, A.A., Cali, T., Brini, M., et al., 2021. Ca(2+) handling at the mitochondria-ER contact sites in neurodegeneration. Cell Calcium 98:102453.

[33] Haase, H., Rink, L., 2014. Multiple impacts of zinc on immune function. Metallomics 6(7):1175—1180.

[34] Wessels, I., Fischer, H.J., Rink, L., 2021. Dietary and physiological effects of zinc on the immune system. Annual Review of Nutrition 41:133—175.

[35] Rodriguez-Calvo, T., Johnson, J.D., Overbergh, L., Dunne, J.L., 2021. Neoepitopes in type 1 diabetes: etiological insights, biomarkers and therapeutic targets. Frontiers in Immunology 12:667989.

[36] Maret, W., 2017. Zinc in pancreatic islet Biology, insulin sensitivity, and diabetes. Preventive Nutrition and Food Science 22(1):1—8.

[37] Ginefra, P., Carrasco Hope, H., Spagna, M., Zecchillo, A., Vannini, N., 2021. Ionic regulation of T-cell function and anti-tumour immunity. International Journal of Molecular Sciences 22(24):13668.